Thin Solid Films 571 (2014) 168–174

Contents lists available at ScienceDirect

Thin Solid Films

journal homepage: www.elsevier.com/locate/tsf

Nanostructuration and band gap emission enhancement of ZnO film via electrochemical anodization

A. Achour [a,*], M.A. Soussou [b,c], K. Ait Aissa [d], M. Islam [e], N. Barreau [d], E. Faulques [d], L. Le Brizoual [f], M.A. Djouadi [d], M. Boujtita [g]

[a] LAAS (CNRS), 7 Avenue du Colonel Roche, 31400 Toulouse, France
[b] LaPhyMNE, University of Gabes, Cité Erriadh, 6072 Zrig, Gabes, Tunisia
[c] IC2MP, UMR 7285, University of Poitiers, 4 Rue Michel Brunet, 86022 Poitiers, France
[d] Institut des Matériaux Jean Rouxel, Université de Nantes, CNRS, 2 Rue de la Houssinière BP 32229, 44322, Nantes Cedex 3, France
[e] College of Engineering, King Saud University, P.O. Box 800, Riyadh 11421, Saudi Arabia
[f] University of Rennes 1, Institut d'Electronique et de Télécommunications, IETR — UMR CNRS 6164, Campus de Beaulieu — Bat 11D 263 Av General Leclerc, 35042 Rennes Cedex, France
[g] CEISAM, Université de Nantes, CNRS, 2 Rue de la Houssiniere, BP 32229, 44322 Nantes Cedex 3, France

ARTICLE INFO

Article history:
Received 20 January 2014
Received in revised form 9 October 2014
Accepted 17 October 2014
Available online 22 October 2014

Keywords:
Zinc oxide
Thin films
Anodic oxidation
Photoluminescence
Band gap emission

ABSTRACT

We report fabrication of nanostructured zinc oxide (ZnO) thin films with improved optical properties through electrochemical anodization. The ZnO films were produced over silicon substrates via radio-frequency (RF) plasma magnetron sputtering technique followed by electrochemical treatment in potassium sulfate solution. After electrochemical treatment, the effect of applied potential on the band gap emission behavior of ZnO films was investigated for the potential drop of 1.8, 2.4 and 3.0 V against reference electrode of Ag/AgCl/0.1 M KCl. Depending on these values, ZnO films with different degrees of nonporous morphology, improved structural quality and oxygen-rich surface chemistry were obtained. The treatment also resulted in enhancement of band gap emission from ZnO films with the degree of enhancement depending on the applied potential. As compared to the as-deposited films, a maximum increase in the photoemission intensity by more than 2.2 times was noticed. In this paper, any changes in the structure, surface chemistry and band gap emission intensity of the RF sputter deposited films, as induced by the anodization treatment at differential potential values, are discussed.

1. Introduction

Zinc oxide (ZnO) is a wide direct band gap semiconductor (3.3 eV) with large exciton binding energy (60 meV) [1]. It is commonly used in various devices such as gas sensors, transparent conducting electrode (TCO) in thin film solar cells, surface acoustic wave and microfluidic applications. Its unique electro-optical properties, particularly, allow its use as ultraviolet (UV) light-emitting diodes and blue luminescent devices [2] and, for this purpose, extensive research efforts are underway to enhance band gap emission characteristics of the ZnO films [1–3]. Nanostructuration of the ZnO films has been reported as one of the possible means to improve its band gap emission and to raise its efficiency as TCO in photovoltaic applications [1,4]. Various morphologies of ZnO nanostructures including nanorods [1,4], nanowalls [5] and single-crystal nanotubes [6] can be synthesized using different methods such as: hydrothermal technique [7], template-assisted growth [8] and ultra-fast microwave method [9]. However, these synthesis routes have disadvantages of (i) poor adhesion to the substrate, making it difficult to integrate them into the device configuration and (ii) presence of structural defects and contaminants inherent in these processing routes, leading to suppression of the UV emission as in the case of photoluminescence (PL), for example [10]. To overcome these limitations, one can deposit ZnO films with good structural quality using vacuum-assisted physical vapor deposition (PVD) techniques. PVD techniques can produce high-purity, uniformly thick, well-adherent ZnO films at relatively low temperature and over large areas with tuneable structural morphology and composition, besides compatibility with micro-fabrication protocol [3]. The ZnO films produced using the PVD process, however, often exhibit dense structural morphology with an associated lower surface-to-volume ratio as compared to their nanostructured counterparts, thus limiting their performance in certain applications [4].

In this work, the benefits from sputter deposition of ZnO and their subsequent nanostructuration are combined by devising a simple, cost-effective approach towards fabrication of nanoporous ZnO films from dense ZnO film structures prepared using RF-plasma magnetron sputtering. The fabrication of such ZnO nanostructures was achieved through applying electrochemical anodization in a non-toxic and environment-friendly electrolyte solution of potassium sulfate (K_2SO_4). The ZnO nanostructures so obtained preserve their good adhesion to the substrate, while their structural quality can even be further

* Corresponding author. Tel./fax: +33 02423968.
E-mail address: a_aminph@yahoo.fr (A. Achour).

http://dx.doi.org/10.1016/j.tsf.2014.10.061
0040-6090/

improved. Furthermore, the nanostructures exhibit enhanced band gap emission at room temperature.

In fact, the electrochemical treatment of ZnO has been reported by some groups. For example, Pust et al. [11] reported on the change of the surface morphology of RF-sputtered ZnO:Al thin films by means of an anodic electrochemical treatment in hydrochloric acid solution, for application as a front contact in Si thin film solar cells. In this work, the treatment of ZnO films in K_2SO_4 solution allows the nanostructuration of the ZnO not only at the surface region, as reported by Pust et al. [11], but also at the bulk region. In this paper, the correlation between morphology and surface chemistry of the ZnO films with band gap emission intensity enhancement, before and after electrochemical cycling, is also discussed.

2. Experimental

2.1. ZnO films deposition

Using the RF-plasma magnetron sputtering system, ZnO films with thickness of ~550 nm were deposited over silicon (100) substrate at room temperature. For this purpose, a disk-shaped ZnO target (>99.9% purity, 4 in. diameter) and argon gas (99.99%) were employed as sputtering target and gas, respectively, with 350 W applied power. More details on the experimental setup are described elsewhere [12].

2.2. Electrochemical anodization

The as-deposited ZnO films (3×1 cm^2 area) were electrochemically treated through anodic polarization at different potential windows in the range of 0–1.8, 0–2.4 or 0–3.0 V vs. SCE at room temperature (25 °C). A non-buffered electrolyte solution of 0.5 M K_2SO_4 (pH ~ 5.5) was prepared by dissolving K_2SO_4 in deionized water without any solution pre-treatment such as preheating to remove dissolved CO_2 before cycling. The electrochemical treatment was performed using a potentiostat/galvanostat (Biologic instrument monitored with ECLab software) with a three-electrode cell configuration consisting of a ZnO film surface, platinum mesh and Ag/AgCl/0.1 M KCl as working electrode, counter electrode and reference electrode, respectively. The scan rate of 20 mV s^{-1} was maintained for a total of 20 cycles in each case. After the electrochemical treatment, the samples were rinsed with deionized water to remove salt residues originating from the electrolyte solution. For sample labeling, the films cycled in the range of 0–1.8, 0–2.4 and 0–3.0 V vs. Ag/AgCl/0.1 M KCl are referred to as films cycled up to 1.8, 2.4 and 3.0 V, respectively.

2.3. Sample characterization

The surface and cross-section morphologies of the ZnO films were examined under scanning electron microscope (JEOL, JSM 7600F) at 5 kV accelerating voltage. For structural analysis, X-ray diffraction (XRD) studies were performed with an X-ray diffractometer (Siemens D5000) employing monochromatic CuKα radiation ($\lambda = 1.5404$ Å) in Bragg Brentano and Rocking curve configurations. Photoluminescence (PL) measurements were made on a Jobin-Yvon Fluorolog 3 spectrometer using a Xenon lamp (500 W) with excitation wavelength of 300 nm at room temperature. X-ray photoelectron spectroscopy (XPS) measurements were carried out on a Kratos Axis Ultra using Al Kα (1486.6 eV) radiation. The C1s line of 284.4 eV was used as a reference to correct the binding energies for charge energy shift. The Shirley background was subtracted from the spectra, whereas signal symmetric Gaussian functions were used in the peak fitting procedures.

3. Results and discussion

In a preliminary study, we examined a series of cyclic voltammograms (CV) carried out for the ZnO film electrodes in the range of 0–3.0 V vs Ag/AgCl/0.1 M KCl at 20 mV s^{-1} scan rate. The first scan of potential (Fig. 1) displays a well-defined anodic peak at about 1.8 V while after the 20th scan of potential, a significant change in the shape of the curve is observed, indicative of an electrochemical process involving the ZnO film surface [13]. In other words, the peak intensity experiences a progressive reduction with an increase in the number of scan cycles. Moreover, the rate of anodic dissolution of the ZnO materials, in both acidic and alkaline baths, has been reported to be higher than that in solutions with 7–8 pH [14,15]. At these high potential values (Fig. 1), the oxygen evolution reaction (Eq. 1) is supposed to be expected, leading to a localized increase in the proton concentration in the vicinity of the ZnO electrode. This may facilitate the chemical dissolution of the ZnO film via Eq. 3. Thus, there are two competing reactions involving ZnO film dissolution, as described below [11,16–18]:

$$2\,ZnO \rightarrow 2Zn^{2+} + O_2 + 4e^- \quad (1)$$

$$2H_2O \rightarrow 4H^+ + O_2 + 4e^- \quad (2)$$

$$2\,ZnO + 4H^+ \rightarrow 2ZnOH^+ + 2H^+ \rightarrow 2Zn^{2+} + 2H_2O. \quad (3)$$

The effect of the potential range on the cross-section morphologies of the etched films was then examined. SEM images of ZnO film cross-sections, before and after the electrochemical anodic dissolution in various potential values namely in the range of 0–1.8, 0–2.4 and 0–3.0 V, are shown in Fig. 2 a–d, respectively. The as-deposited ZnO film (Fig. 2a) shows dense columnar morphology with surface roughness originating from growth and subsequent impingement of neighboring islands during the film deposition. After the electrochemical treatment, the ZnO surface becomes rougher, while the columnar structure becomes more pronounced as the applied potential value increases from 1.8 to 3.0 V, as manifested in Fig. 2(b–d). The increase in film roughness is due to the fact that the film surfaces become nano-porous after electrochemical treatment.

The porosity was also found to increase with an increase in the applied potential window, as shown in Fig. 3, where anodization of the films at 1.8, 2.4 or 3.0 V causes formation of highly nanoporous ZnO films in the form of inter-connected nano islands. It must be noted that the film thickness was not affected by the electrochemical treatments at different applied potentials. The SEM images of the ZnO film surfaces (Fig. 3a–d) confirm that the columnar structure, observed after cycling, is due to the formation of nano-channels along the film

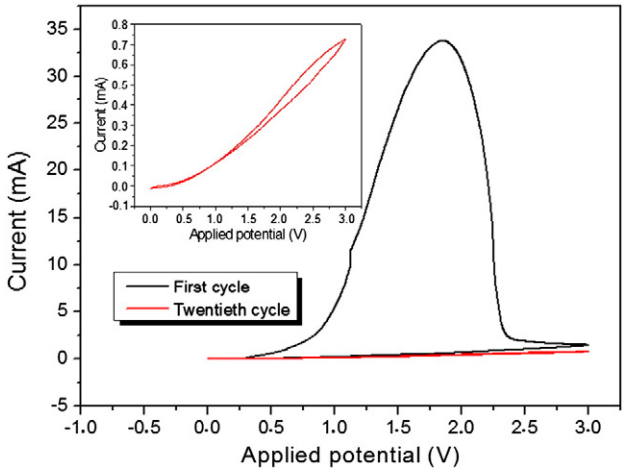

Fig. 1. Effect of cycle number on the shape of cyclic voltammetric curves at potential window of 0–3 V. For more clarity, we display only the first and 20th cyclic voltammetric curves of ZnO film carried out in K_2SO_4 (0.5 M) solution at scan rate of 20 mV s^{-1}.

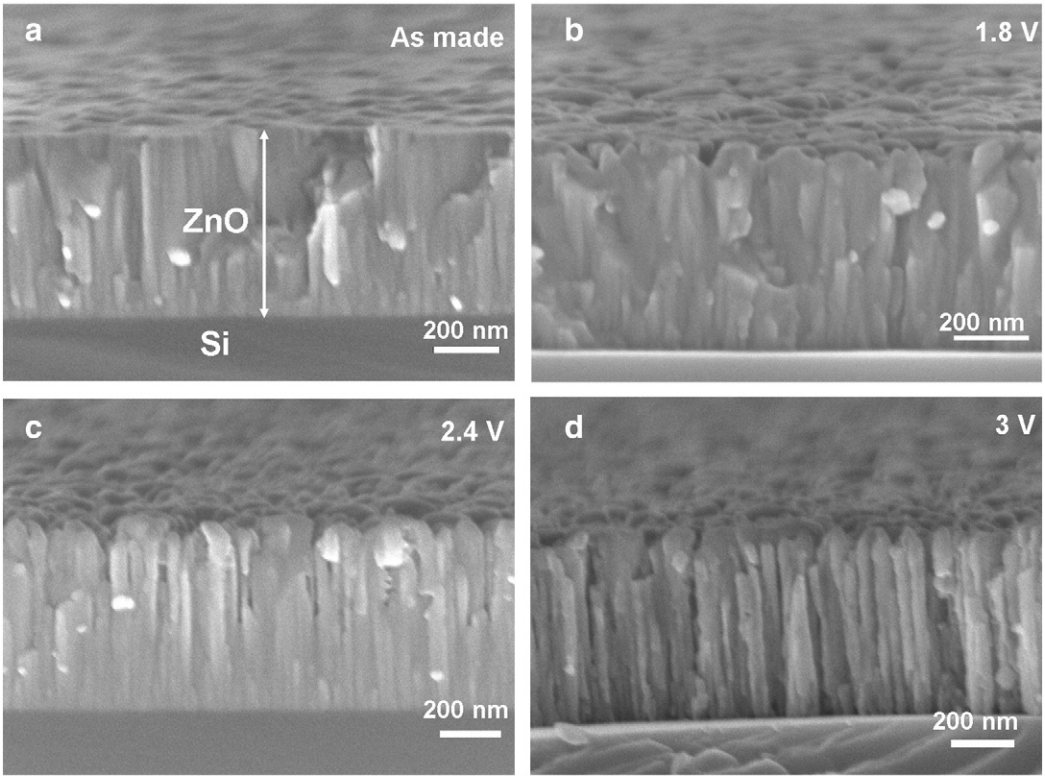

Fig. 2. Side view SEM images of ZnO films (a) before electrochemical treatment and after electrochemical treatment at potential windows of (b) 0–1.8 V, (c) 0–2.4 V and (d) 0–3 V.

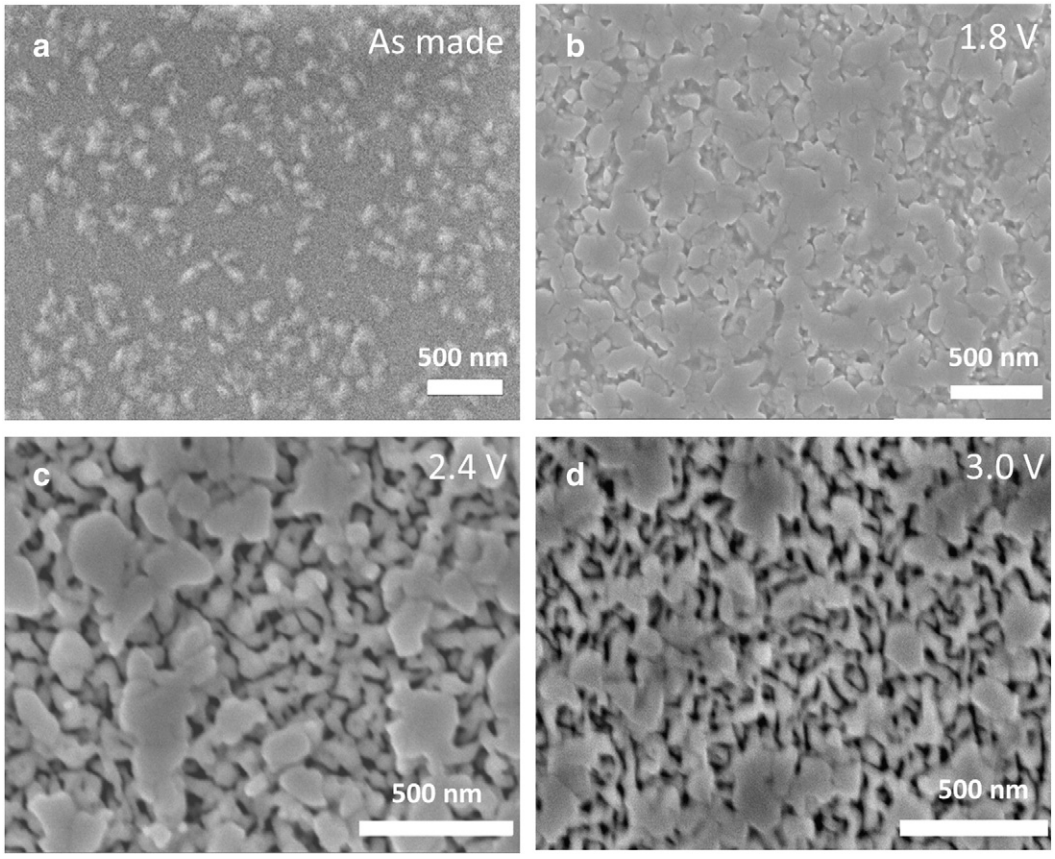

Fig. 3. Top view SEM images of ZnO films (a) before electrochemical treatment and after electrochemical treatment at potential windows of (b) 0–1.8 V, (c) 0–2.4 V and (d) 0–3 V.

thickness. These channels reach the bottom of the films upon increasing the applied potential from 1.8 up to 3.0 V, as evident from Fig. 2d. Therefore, the ZnO nanostructuration is not only limited to the film surface but also to the bulk region. The films showed good adhesion to the silicon substrate even after scratching with a diamond tip.

The mechanism of nanoporosity formation in ZnO films can be attributed to localized corrosion at grain boundaries, triggered by the reaction of ZnO film surface with etching agents in the electrolyte solution [11,19]. The ZnO etching behavior can be explained by the wurtzite structure and the dangling bond model, described in Ref [19]. In ZnO, the surface atoms on the perfect polar faces are tightly bound to three neighboring atoms from the bulk material, while the atoms in the underlying layer are bound to only one atom in the bulk. Thus, the etching step is to remove the tightly bound top atom. The partial positive and negative charges of the dangling bonds at the Zn(001) and O(001) terminated surfaces can easily be attacked by hydronium (H_3O^+) ions that come from oxygen evolution reaction (Eq. 2). In this case, the attack of etching species can only occur at the defects such as screw dislocations where the charge repulsion is disrupted. It is noteworthy that our simple process can be used to fabricate uniform nanoporous ZnO films at room temperature with good adhesion to the substrate and without any need for surfactants or a template. The porosity so produced is expected to affect both electrical and optical characteristics of the films.

Before and after the electrochemical treatment, the ZnO films show single preferential orientation along the c-axis, as confirmed by the XRD pattern (Fig. 4a), through the presence of a distinct (0002) peak characteristic of the wurtzite structure of the ZnO. The shift in the (0002) peak position towards higher 2θ values in the case of ZnO films anodized at 2.4 and 3.0 V is by ~0.12 and 0.14°, respectively. This shift suggests relaxation of compressive stresses presumably due to the formation of a porous structure [20,21]. The full-width-at-half-maximum (FWHM) value of X-ray diffraction ώ rocking measurement of the (0002) plane of the as-prepared ZnO film is 2.8°. After electrochemical cycling, the FWHM value decreases to 2.6, 2.5 and 2.2° for the films cycled in applied potential values of 1.8, 2.4 and 3.0 V, respectively. Since XRD is a bulk characterization technique, the decrease in the FWHM value upon increasing the applied potential also confirms etching of the film within the bulk region. Indeed, the decrease of FWHM could be attributed to the relaxation of compressive stresses and/or the improvement of structural quality through removal of defective and less oriented (0002) grains at the boundaries during electrochemical etching. This is in good agreement with the model proposed by Hüpkes et al. [19] who reported that attack of the etching species can only occur at defects such as screw dislocations present in the ZnO.

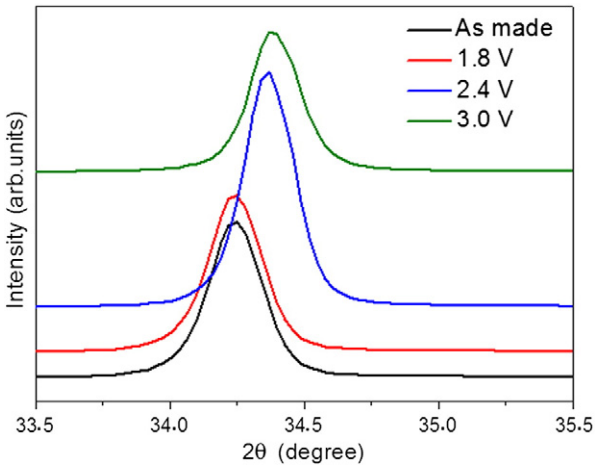

Fig. 4. XRD patterns of ZnO films before and after electrochemical treatment.

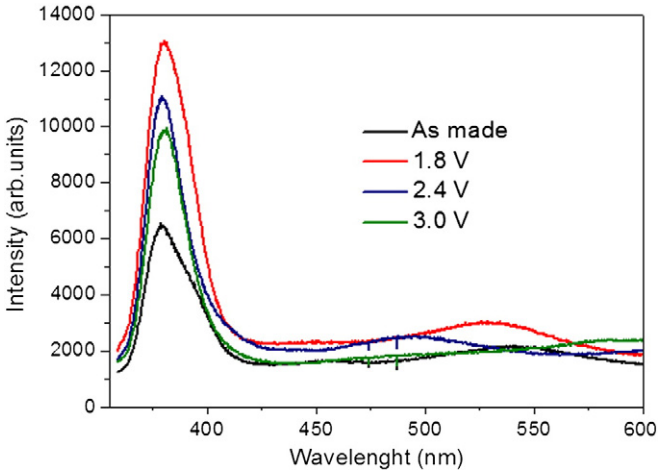

Fig. 5. PL spectra of ZnO films before and after electrochemical treatment.

The room temperature PL analysis of ZnO films, before and after treatment at applied potential of 1.8 up to 3.0 V, is shown in Fig. 5. The band at ~377. 2 nm, which corresponds to ~3.3 eV energy, is attributed to the band gap emission in ZnO [22]. The defect emissions due to structural defects in ZnO (oxygen vacancies, Zn interstitial, etc.) are usually located in the spectral range of 450–650 nm [23]. From Fig. 5, it is evident that although these defects are present in the as-deposited ZnO film, their intensities are very low compared to the band gap emission intensity, indicating good crystalline quality of the film. The electrochemical treatment led to an enhancement of the band gap emission intensity in ZnO by ~2.2, 1.8 and 1.6 fold for ZnO cycled under applied potential values in the range of 0–1.8, 0–2.4 and 0–3.0 V, respectively. The 2.2 fold intensity enhancement for ZnO cycled at 1.8 V is comparable to that of ZnO buffered with TiN [12]. This degree of enhancement is also comparable to that of ZnO-coated multi-walled carbon nanotubes (3-fold enhancement) reported earlier [8]. Furthermore, when compared to other published results, the room temperature PL intensity enhancement for our electrochemically treated ZnO films is competitive with that of ZnO buffered with MgF_2 (four folds) [24], ZnO layer (two folds) [25] and Al_2O_3 (58%) [26], whereas it is much higher than that of ZnO buffered with SiO_2 and S_3iN_4 [27]. It should be noted that despite the improvement in the band gap emission of ZnO film treated at 1.8 V, the PL curve shows defect emission at around 530 nm which is attributed to Zn interstitials [28].

The enhancement of the band gap emission intensity maybe attributed to the change in the structural morphology and stress relaxation in the films after electrochemical cycling. It is a well-known fact that relaxation of compressive stresses in ZnO and improvement in its structural quality lead to improved optical properties in terms of enhancement of its band gap emission [29,30]. In the present work, the observed enhancement may be partially assigned to the improvement in structural quality as can be deduced from the decrease of the rocking curve value after film treatment. Another contributing factor may be the relaxation of compressive stresses in the films after anodization (Fig. 4a) besides an increase in the surface area, as suggested in the case of ZnO deposition on carbon nanotubes [8]. However, these are not the only parameters involved since the ZnO film that shows the highest enhancement intensity (cycled at 1.8 V) shows less relaxation of compressive stress and less porosity compared to the films treated at 2.4 and 3.0 V (Fig. 2). Therefore, the surface chemistry of ZnO should have an important role towards enhancement of the band gap emission intensity.

In order to elucidate the PL emission behavior, XPS analysis was performed on ZnO films before and after electrochemical treatment. The XPS Zn 2p and O 1s high resolution spectra of as-deposited and electrochemically treated (at 1.8, 2.4 and 3.0 V) ZnO films are presented in

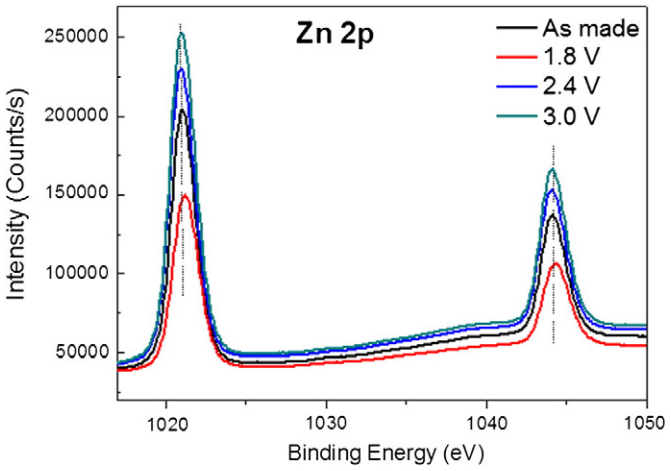

Fig. 6. XPS Zn 2p core level spectra from ZnO surface before and after electrochemical treatment.

Figs. 6 and 7, respectively. The Zn 2p spectra show that the binding energy (BE) value of the ZnO film, upon treatment at 1.8 V, experiences a slight shift by 0.2 eV towards higher value with respect to those of as-deposited and electrochemically treated (2.4 and 3.0 V) ZnO films, indicating that a higher number of Zn atoms are bound to the O atoms in ZnO after treatment at 1.8 V [31]. In other words, this shift may be caused by a decrease in the oxygen vacancy concentration. The O 1s peak of ZnO is usually fitted by three nearly Gaussian components centered at ~530.5, 531.6 and 532.7 eV [32–38]. In this study, the O 1s peak on the surface of as-deposited ZnO film maybe fitted with three Gaussians O_1, O_2 and O_3 centered at 529.8, 530.8 and 531.7 eV, while the O 1s on the ZnO film surface, treated at 1.8, 2.4 and 3.0 V, can be fitted with three Gaussians as well, as shown in Fig. 7. The O_1 component on the low binding energy side of the O 1s spectrum is attributed to the Zn–O bonds, in the wurtzite structure of the hexagonal Zn^{2+} ion array, surrounded by Zn atoms with full supplement of the nearest-neighbor O^{2-} ions. The intermediate O_2 is due to O^{2-} ions in the oxygen deficient regions within the ZnO matrix, while the high binding energy component O_3 is usually attributed to the presence of loosely bound oxygen on the surface, chemisorbed or dissociated oxygen or OH species on the surface of the ZnO thin film and other species such as H_2O, O_2, H and CO_3 [32–38]. Therefore, the intensity of the O_1 component is a measure of the number of oxygen atoms in a fully oxidized stoichiometric surrounding, whereas intensity of the O_2 component can be in connection with variations in the oxygen vacancy concentration. Table 1 presents the peak positions of O_1, O_2 and O_3 with their respective percentages. The shift of these peaks towards lower or higher BE values, with respect to those of as-deposited ZnO film, may be due to the difference in stoichiometry, nature and degree of interaction with various chemisorbed and/or physisorbed species.

It can be seen from Table 1 and Fig. 7 that the ZnO film surface, after electrochemical treatment at 1.8 V, contains less amount of oxygen vacancies (O_2 component percentage) as compared to other films investigated in this study which is in agreement with PL analysis (Fig. 5) which recorded an increase in the Zn interstitial defect signal after treatment at this potential. The percentage of oxygen vacancies in ZnO treated at 1.8 V can be estimated to be 7% versus 16, 22 and 24% for the as-deposited and electrochemically treated (at 2.4 and 3.0 V) ZnO films, respectively. It is also noticed that the percentage of O_3, attributed to loosely bound oxygen on the surface, chemisorbed or dissociated oxygen or OH species on the surface, has the highest intensity after film treatment at 1.8 V. This explains the very low amount of oxygen

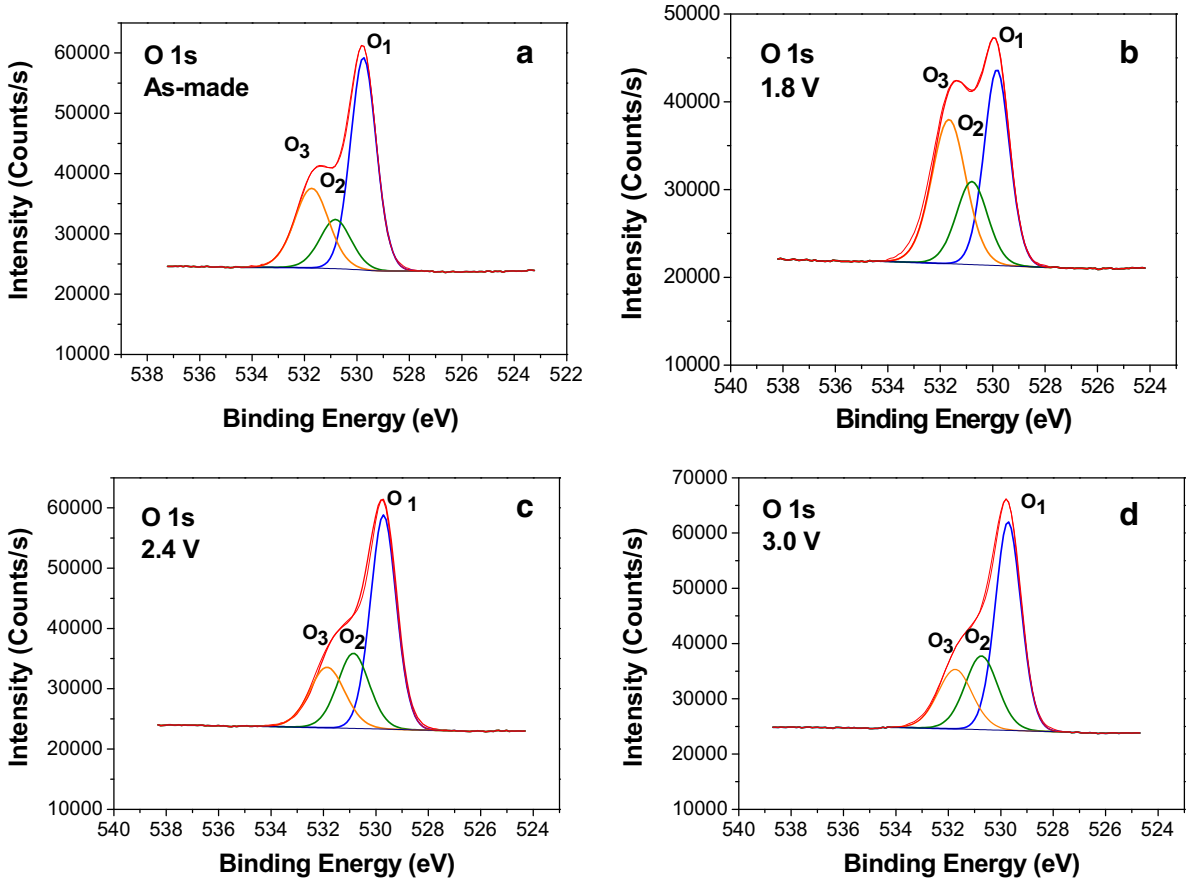

Fig. 7. XPS O 1s deconvoluted core level spectra of (a) as prepared ZnO film and ZnO film treated at potential windows of (b) 0–1.8 V, (c) 0–2.4 V and (d) 0–3 V.

Table 1
The three O 1s components of ZnO films before and after treatment, their FWHM and percentage.

Film	O 1s binding energy (eV)	FWHM (eV)	Percentage (%)
As made	O_1: 529.8	1. 1	56
	O_2: 530.8	1.4	16
	O_3: 531.7	1.5	28
1.8 V	O_1: 529.8	1.1	43
	O_2: 530.9	1.4	7
	O_3: 531.6	1.5	50
2.4 V	O_1: 529.7	1.1	59
	O_2: 531.0	1.4	22
	O_3: 531.9	1.5	19
3 V	O_1: 529.7	1.1	56
	O_2: 531.0	1.5	24
	O_3: 531.9	1.5	20

vacancies in this film. In fact, the oxygen vacancies in the film treated at 1.8 V are supposed to be healed by O or OH adsorption during the potential cycling in the aqueous solution, as has been demonstrated in the case of other types of semiconductor materials [39], and this has been found to have a considerable effect on the PL properties of ZnO. Indeed, the low amount of oxygen vacancies in the ZnO film leads to an enhancement of the band gap emission [40,41]. Moreover it has been reported in the literature that healing of oxygen vacancies by surface oxidation of ZnO surface promotes improvement in its optical properties [40–42]. This can explain the highest intensity of PL obtained in the case of ZnO film treated at 1.8 V, although this film has moderate surface area compared to the other films treated at 2.4 and 3.0 V.

The surface oxidation/or oxygen vacancy healing seem to be insufficient in the case of films cycled up to 2.4 and 3.0 V. In fact, the amount of oxygen vacancies has increased in these cases. Their PL intensities, however, remain higher than those of the as-deposited film which contains less concentration of oxygen vacancies at its surface region. This can be attributed to the surface area effect which is more important in the case of films treated at 2.4 and 3.0 V. Therefore, the band gap emission intensity in the ZnO films should be considered to have been caused by two competing factors namely the film surface chemistry and the film surface area.

Conclusion

In summary, we presented a simple, cost effective approach to enhance the band gap emission intensity of RF-plasma sputtered ZnO films by means of an anodic electrochemical treatment in K_2SO_4 electrolyte solution. The enhancement intensity increases by more than 2.2 folds upon electrochemical treatment at 1.8 V. Besides changes in morphology and improvement in the surface crystalline quality of the films after the electrochemical treatment, the surface chemistry of the treated films has considerable effect on the UV emission enhancement. It was found that a reduction in the oxygen vacancy concentration in the ZnO film surface has a more predominant role than an increase in the surface area towards enhancement of the UV emission characteristics. Moreover, the electrochemical treatment allowed the fabrication of ZnO nanostructures in the form of nanoporous films at room temperature and with good interfacial adhesion to the substrate without any need for surfactants. Such nanoporous ZnO films can be beneficial for application in Si thin film solar cells and photocatalysis.

Acknowledgments

The authors would like to thank N. Stephant and S. Grolleau (IMN, Nantes) for their help during SEM studies. The authors also appreciate assistance from V. Fernandez and J. Hammon (IMN, Nantes) with XPS analysis. The authors would like to extend their sincere appreciation to the Deanship of Scientific Research at King Saud University for its funding of this research through the Research Group Project no. RGP-VPP-283.

References

[1] Z.L. Wang, Zinc oxide nanostructures: growth, properties and applications, J. Phys. Condens. Matter 16 (2004) R829.
[2] A. Janotti, C.G.V.d. Walle, Fundamentals of zinc oxide as a semiconductor, Rep. Prog. Phys. 72 (2009) 126501.
[3] S. Rahmane, B. Abdallah, A. Soussou, E. Gautron, P.Y. Jouan, L. Le Brizoual, N. Barreau, A. Soltani, M.A. Djouadi, Epitaxial growth of ZnO thin films on AlN substrates deposited at low temperature by magnetron sputtering, Phys. Status Solidi A 207 (2010) 1604.
[4] L. Schmidt-Mende, J.L. MacManus-Driscoll, ZnO — nanostructures, defects, and devices, Mater. Today 10 (2007) 40.
[5] M.Q. Israr, J.R. Sadaf, O. Nur, M. Willander, S. Salman, B. Danielsson, Chemically fashioned ZnO nanowalls and their potential application for potentiometric cholesterol biosensor, Appl. Phys. Lett. 98 (2011) 253705.
[6] S.L. Mensah, V.K. Kayastha, I.N. Ivanov, D.B. Geohegan, Y.K. Yap, Formation of single crystalline ZnO nanotubes without catalysts and templates, Appl. Phys. Lett. 90 (2007) 113108.
[7] S. Baruah, J. Dutta, Hydrothermal growth of ZnO nanostructures, Sci. Technol. Adv. Mater. 10 (2009) 013001.
[8] N. Ouldhamadouche, A. Achour, I. Musa, K. Ait Aissa, F. Massuyeau, P.Y. Jouan, M. Kechouane, L. Le Brizoual, E. Faulques, N. Barreau, M.A. Djouadi, Structural and photoluminescence characterization of vertically aligned multiwalled carbon nanotubes coated with ZnO by magnetron sputtering, Thin Solid Films 520 (2012) 4816.
[9] N. Tabet, R. Al Ghashani, S. Achour, Ultra fast synthesis of zinc oxide nanostructures by microwaves, Superlattice. Microst. 45 (2009) 598.
[10] K.H. Tam, C.K. Cheung, Y.H. Leung, A.B. Djurišić, C.C. Ling, C.D. Beling, S. Fung, W.M. Kwok, W.K. Chan, D.L. Phillips, L. Ding, W.K. Ge, Defects in ZnO nanorods prepared by a hydrothermal method, J. Phys. Chem. B 110 (2006) 20865.
[11] S.E. Pust, J.-P. Becker, J. Worbs, S.O. Klemm, K.J.J. Mayrhofer, J. Hüpkes, Electrochemical etching of zinc oxide for silicon thin film solar Cell Applications, J. Electrochem. Soc. 158 (2011) D413.
[12] A. Achour, K.A. Aissa, M. Mbarek, K. El Hadj, N. Ouldhamadouche, N. Barreau, L. Le Brizoual, M.A. Djouadi, Enhancement of near-band edge photoluminescence of ZnO film buffered with TiN, Thin Solid Films 538 (2013) 71.
[13] M. Pourbaix, Atlas of Electrochemical Equilibria in Aqueous Solutions, National Association of Corrosion Engineers, Houston, TX1974. 411.
[14] M. Valtiner, S. Borodin, G. Grundmeier, Stabilization and acidic dissolution mechanism of single-crystalline ZnO(0001) surfaces in electrolytes studied by in-situ AFM imaging and ex-situ LEED, Langmuir 24 (2008) 5350.
[15] H. Gerischer, N. Sorg, Chemical dissolution of zinc oxide crystals in aqueous electrolytes — an analysis of the kinetics, Electrochim. Acta 37 (1992) 827.
[16] Z. Zembura, L. Burzynska, The corrosion of zinc in de-aerated 0.1 M NaCl in the pH range from 1.6 to 13.3, Corros. Sci. 17 (1977) 871.
[17] B. Pettinger, H.R. Schöppel, T. Yokoyama, H. Gerischer, Ber. Bunsenges. Phys. Chem. 78 (1974) 1024.
[18] J.-P. Becker, S.E. Pust, J. Hüpkes, Effects of the electrolyte species on the electrochemical dissolution of polycrystalline ZnO:Al thin films, J. Electrochem. Acta 112 (2013) 976.
[19] J. Hüpkes, J.I. Owen, S.E. Pust, E. Bunte, Chemical etching of zinc oxide for thin-film silicon solar cells, Chem. Phys. Chem. 13 (2012) 66.
[20] V. Lysenko, D. Barbier, B. Champagnon, Stress relaxation effect in porous 3C-SiC/Si heterostructure by micro-Raman spectroscopy, Appl. Phys. Lett. 79 (2001) 2366.
[21] M. Mynbaeva, A. Titkov, A. Kryganovskii, V. Ratnikov, K. Mynbaev, H. Huhtinen, R. Laiho, V. Dmitriev, Structural characterization and strain relaxation in porous GaN layers, Appl. Phys. Lett. 76 (2000) 1113.
[22] R. Macaluso, M. Mosca, C. Calì, F. Di Franco, M. Santamaria, F. Di Quarto, J.-L. Reverchon, Erroneous *p*-type assignment by Hall effect measurements in annealed ZnO films grown on InP substrate, J. Appl. Phys. 113 (2013) 164508.
[23] T.M. Børseth, B.G. Svensson, A.Y. Kuznetsov, P. Klason, Q.X. Zhao, M. Willander, Identification of oxygen and zinc vacancy optical signals in ZnO, Appl. Phys. Lett. 89 (2006) 262112.
[24] R. Hong, J. Shao, H. He, Z. Fan, Enhancement of near-band edge photoluminescence of ZnO thin films by employing MgF2 buffer layer, J. Cryst. Growth 290 (2006) 334.
[25] J. Zhao, L. Hu, Improvement in crystal quality of ZnO film on Si substrate by using a homo-buffer layer, Mater. Sci. Semicond. Process. 12 (2009) 233.
[26] T. Wang, H. Wu, C. Chen, C. Liu, Growth, optical, and electrical properties of nonpolar m-plane ZnO on p-Si substrates with Al_2O_3 buffer layers, Appl. Phys. Lett. 100 (2012) 011901.
[27] C.-C. Lin, S.-Y. Chen, S.-Y. Cheng, PL dependence of ZnO films grown on Si with various buffer layers by RF magnetron sputtering, Electrochem. Solid-State Lett. 7 (2004) J20.
[28] K.Y. Wu, Q.Q. Fang, W.N. Wang, C. Zhou, W.J. Huang, J.G. Li, Q.R. Lv, Y.M. Liu, Q.P. Zhang, H.M. Zhang, Influence of nitrogen on the defects and magnetism of ZnO:N thin films, J. Appl. Phys. 108 (2010) 063530.
[29] S.Y. Hu, Y.C. Lee, J.W. Lee, J.C. Huang, J.L. Shen, W. Water, The structural and optical properties of ZnO/Si thin films by RTA treatments, Appl. Surf. Sci. 254 (2008) 1578.
[30] J.B. You, X.W. Zhang, Y.M. Fan, Z.G. Yin, P.F. Cai, N.F. Chen, Effects of crystalline quality on the ultraviolet emission and electrical properties of the ZnO films deposited by magnetron sputtering, Appl. Surf. Sci. 255 (2009) 5876.
[31] J. He, B. Tan, Y. Su, S. Yang, Q. Wei, XPS analysis of ZnO thin films obtained by pulsed laser deposition, Adv. Mater. Res. 383 (2012) 6293.

[32] H.T. Cao, Z.L. Pei, J. Gong, C. Sun, R.F. Huang, L.S. Wen, Preparation and characterization of Al and Mn doped ZnO (ZnO: (Al, Mn)) transparent conducting oxide films, J. Solid State Chem. 177 (2004) 1480.
[33] P.T. Hsieh, Y.C. Chen, K.S. Kao, C.M. Wang, Luminescence mechanism of ZnO thin film investigated by XPS measurement, Appl. Phys. A 90 (2008) 317.
[34] H. Wagata, N. Ohashi, K.I. Katsumata, K. Okada, N. Matsushita, The effect of citric ion on the spin-sprayed ZnO films: IR and XPS study for the organic impurities, Key Eng. Mater. 485 (2011) 291.
[35] X. Li, Y. Wang, W. Liu, G. Jiang, C. Zhu, Study of oxygen vacancies' influence on the lattice parameter in ZnO thin film, Mater. Lett. 85 (2012) 25.
[36] M. Chen, X. Wang, Y.H. Yu, Z.L. Pei, X.D. Bai, C. Sun, R.F. Huang, L.S. Wen, X-ray photoelectron spectroscopy and auger electron spectroscopy studies of Al-doped ZnO films, Appl. Surf. Sci. 158 (2000) 134.
[37] D. Park, Y. Tak, J. Kim, K. Yong, Low-temperature synthesized ZnO nanoneedles: XPS and PL analysis, Surf. Rev. Lett. 14 (2007) 1061.
[38] Y. Chen, N. Jyoti, K. Hyun-U, J. Kim, Effect of annealing temperature on the characteristics of ZnO thin films, J. Phys. Chem. Solids 73 (2012) 1259.
[39] A. Achour, J.B. Ducros, R.L. Porto, M. Boujtita, E. Gautron, L. Le Brizoual, M.A. Djouadi, T. Brousse, Hierarchical nanocomposite electrodes based on titanium nitride and carbon nanotubes for micro-supercapacitors, Nano Energy 7 (2014) 104.
[40] S.S. Kurbanov, G.N. Panin, T.W. Kim, T.W. Kang, Impact of visible light illumination on ultraviolet emission from ZnO nanocrystals, Phys. Rev. B 78 (2008) 045311.
[41] L. Qin, C. Shing, S. Sawyer, P.S. Dutta, Enhanced ultraviolet sensitivity of zinc oxide nanoparticle photoconductors by surface passivation, Opt. Mater. 33 (2011) 359.
[42] C. Chen, Y. Lu, H. He, M. Xiao, Z. Wang, L. Chen, Z. Ye, Violet emission in ZnO nanorods treated with high-energy hydrogen plasma, Appl. Mater. Interfaces 5 (2013) 10274.